J|A|C|S
ARTICLES
Published on Web 02/23/2007

Autoassembly of Nanofibrous Zeolite Crystals via Silicon Carbide Substrate Self-Transformation

Svetlana Ivanova, Benoit Louis,* Marc-Jacques Ledoux, and Cuong Pham-Huu

Contribution from the Laboratoire des Matériaux, Surfaces et Procédés pour la Catalyse, a member of ELCASS (European Laboratory for Catalysis and Surface Science), CNRS-ULP, 25 rue Becquerel, 67087 Strasbourg Cedex 2, France

Received December 1, 2006; E-mail: blouis@chimie.u-strasbg.fr

Abstract: ZSM-5 zeolite nanofibers with a size of 90 nm and lengths up to several micrometers were prepared via in-situ silicon carbide support self-transformation. The morphology and aggregation degree of these zeolite nanofibers could be modified by adjusting the pH conditions, the nature of the mineralizer (OH^- or F^-), or the synthesis duration. The novelty consists of the preparation of zeolite nanowires without the use of any organogelating agent, along with controlled macroscopic shapes (extrudates, foam monolith) for direct use as a structured reactor. Finally, these materials are catalytically active in the conversion of methanol to gasoline range hydrocarbons (MTG process) and hence exhibit the typical solid acidity of zeolitic materials.

Introduction

Zeolites are among the most used heterogeneous catalysts for the petrochemical industry, especially for cracking and alkylation processes.[1−3] Recently, zeolites became valuable catalysts for the synthesis of fine chemicals like fragrances and pharmaceuticals with low waste release compared to the homogeneous mode.[4−6] In addition, the zeolite catalyst can be recovered by means of filtration which represents a cost effectiveness compared to liquid−liquid separations in the case of a homogeneous medium involving Brönsted and Lewis acids.[3]

In general, zeolites contain a large amount of micropores (<2 nm) which can induce diffusion limitations. Hence, secondary reactions can be promoted if the diffusion of reactants and products throughout the zeolite channels and cavities controls the kinetics of the process. Generally, the acidic condensation of the products, leading to the formation of carbon deposits inside the zeolite channels, is the most frequent case of deactivation. To overcome diffusional limitations, several works have been devoted to the reduction of the zeolite crystal size,[7] introduction of mesoporosity,[8] increase of the zeolite pore size, or the use of an inert support to decrease the layer of diffusion.[9−12]

The synthesis of nanocrystalline ZSM-5 zeolite has been recently reported by several groups.[13−16] However, it is quite difficult to separate zeolite nanocrystals (<100 nm) from the reaction medium, and thus specific filtration−centrifugation devices need to be used. Indeed, the small size of these zeolites hinders their use in a fixed-bed configuration because of the pressure drop created along the catalyst bed. The powdered zeolite could also be coated on a macroscopic shape by addition of an inorganic binder (clay, silica, alumina), following extrusion to yield cylindrical pellets. The main drawbacks are the loss of the effective surface area of the zeolite because of the presence of the binder and diffusion limitations. In some cases, the binder could also undergo reaction with the reactants or products leading to a decrease of the overall selectivity.

The use of structured reactors in catalysis has become a major field in catalysis during the past decade.[17] In combination with studies devoted to find new active phase formulations, numerous research has also been focused on the development of structured composites (catalyst + support) to improve the reactor hydrodynamics and, hence, the catalytic performance for several reactions.[17−19] Thus, structured zeolitic catalysts were prepared via a binderless hydrothermal synthesis on metals[11,20−22] or ceramics.[23−28] In spite of a reduced pressure drop, and improved

(1) Corma A. *Chem. Rev.* **1995**, *95*, 559−614.
(2) Weitkamp J. *Solid State Ionics* **2000**, *131*, 175−188.
(3) *Superacids*; Olah, G. A., Prakash, G. K. S., Sommer, J., Eds.; Wiley: New York, 1985.
(4) Hölderich W. F.; van Bekkum H. *Stud. Surf. Sci. Catal.* **1991**, *58*, 631−727.
(5) Hölderich, W. F.; Hesse, M.; Näumann, F. *Angew. Chem.* **1988**, *100*, 232−251.
(6) Hölderich W. F. *Catal. Today* **2000**, *62*, 115−130.
(7) Tosheva L.; Valtchev V. *Chem. Mater.* **2005**, *17*, 2494−2513.
(8) Madsen C.; Jacobsen C. J. H. *Chem. Commun.* **1999**, 673−674.
(9) Wine G.; Matta J.; Tessonnier J. P.; Pham-Huu C.; Ledoux M. J. *Chem. Commun.* **2003**, 530−531.
(10) Basso S.; Tessonnier J. P.; Wine G.; Pham-Huu C.; Ledoux M. J. U.S. Patent 0162649, 2003.
(11) Louis, B.; Reuse, P.; Kiwi-Minsker, L.; Renken, A. *Appl. Catal. A* **2001**, *210*, 103−109.
(12) Zampieri, A.; Colombo, P.; Mabande, G. T. P.; Selvam, T.; Schwieger, W.; Scheffler, F. *Adv. Mater.* **2004**, *16*, 819−822.
(13) van Grieken, R.; Sotelo, J. L.; Menendez, J. M.; Melero, J. A. *Microporous Mesoporous Mater.* **2000**, *39*, 135−147.
(14) Persson, A. E.; Schoeman, B. J.; Sterte, J.; Otterstedt, J. E. *Zeolites* **1995**, *15*, 611−619.
(15) Reding, G.; Mäurer, T.; Kraushaar-Czarnetzki, B. *Microporous Mesoporous. Mater.* **2003**, *57*, 83−92.
(16) Jacobsen, C. J. H.; Madsen, C.; Janssens, T. V. W.; Jakobsen, H. J.; Skibsted, J. *Microporous Mesoporous Mater.* **2000**, *39*, 393−401.
(17) *Structured Catalysts and Reactors*; Cybulski, A., Moulijn, J. A., Eds.; Marcel Dekker: New York, 1998.
(18) Berger, R. J.; Hugh Stitt, E.; Marin, G. B.; Kapteijn, F.; Moulijn, J. A. *Cattech* **2001**, *5*, 30−60.
(19) Kreutzer, M. T.; Kapteijn, F.; Moulijn, J. A. *Catal. Today* **2006**, *111*, 111−118.

heat and mass tranfers when compared to extrudated pellets or powdered microgranules, the industrial applications of these structured materials remain limited. This is either due to the lack of support inertness or to a nonsufficient mechanical and chemical stability.

Silicon carbide exhibits the intrinsic properties which are required to become a valuable candidate as zeolite support: high thermal conductivity and mechanical strength, high resistance toward oxidation, chemical inertness, and ease of shaping.[29,30] All these advantages tend to indicate that SiC support can replace classical supports such as alumina, silica, or carbon, especially in highly endothermic or exothermic reactions.[29−31]

The aim of the present article is to report the synthesis of ZSM-5 crystals directly grown from the silicon carbide surface as a catalyst for petrochemical applications. Several different strategies have been employed to allow the zeolite to grow including direct growth,[32] template-assisted methods,[33] or self-assembly.[34,35] Recently, silicalite-1 nanocrystals have been used as building blocks to prepare organized zeolite structures, such as thin films and fibers.[7] One can expect that the formation of films or fibers will improve the efficiency of zeolites in many current applications and will open the door to new kinds of investigation. Moreover, it is expected that the combination of the high thermal conductivity of silicon carbide and the one-dimensional zeolite network could give rise to a new kind of nanomaterial with interesting catalytic properties. The methanol-to-gasoline (MTG) reaction was chosen as a test reaction, since the size and shape of the zeolite crystals, together with the methanol partial pressure and the residence time, govern the selectivity toward light olefins or saturated hydrocarbons.[36]

Experimental Section

β-SiC Support Characteristics. Silicon carbide was prepared by the gas−solid reaction between solid carbon and SiO vapors in the temperature range 1200−1400 °C according to the shape memory synthesis developed by Ledoux et al.[29−31] This method allows the synthesis of silicon carbide with different sizes and shapes, depending on their subsequent uses, and having specific surface areas (SSA) up to 150 m^2/g. SiC was used in its β-crystalline structure since the SSA is higher than the one from α-SiC.[30] Figure 1 presents the β-SiC macroscopic shapes used: extrudated pellets (2 × 6 mm in size) or open-cell foams (25 × 40 mm in size). Prior to the synthesis, the support was calcined at 900 °C for 2 h to form a nanoscopic layer of SiO_2 on its surface (10 wt %). This layer will provide the reservoir of nutrient SiO_2 for the zeolite synthesis. Figure 1 also presents a scanning electron microscopy (SEM) micrograph of the silicon carbide surface.

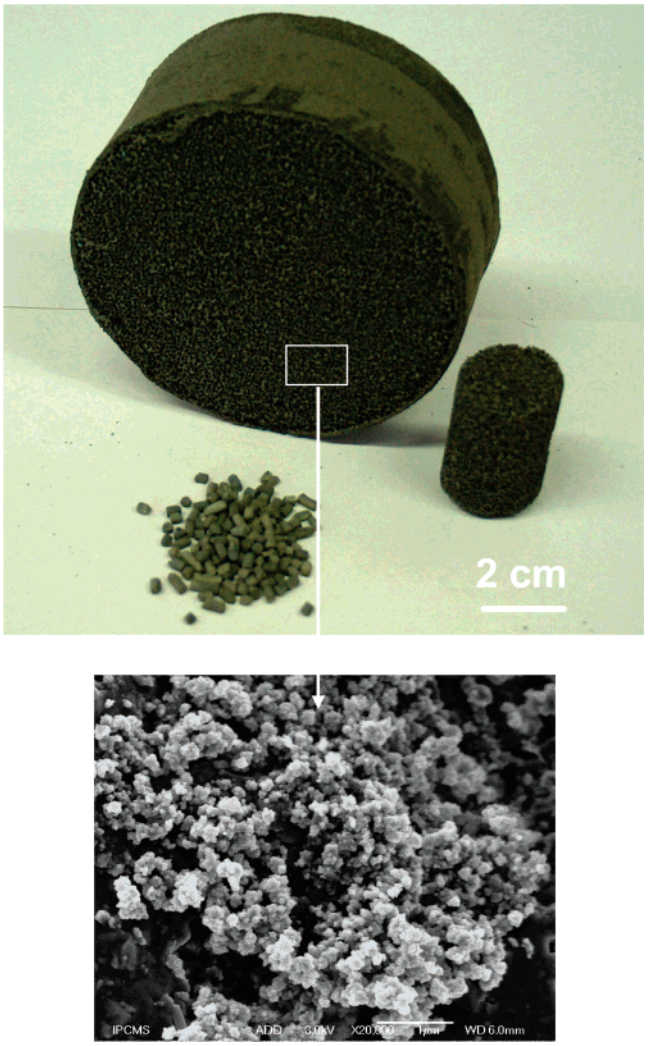

Figure 1. β-SiC macroscopic shapes: extrudated pellets and different open-cell foams (a). High-resolution SEM image of the SiC surface (b).

Zeolite Coating Preparation. The SiC support (6 g, extrudates or foams) was placed in a Teflon-lined stainless steel autoclave (70 mL) filled with 50 mL of the synthesis mixture.

Hydroxide-Mediated Route. The synthesis mixture was prepared by mixing deionized water and template (TPAOH 1M, Sigma-Aldrich) and by stirring for 10 min. The precursor solution was achieved by stirring the mixture after an addition of sodium hydroxide (NaOH, 98%, Fluka) for 15 min. Then, sodium aluminate ($NaAlO_2$, Riedel de Häen) was added and the solution was stirred for another 15 min. The reactants were mixed according to the following composition: $NaAlO_2$:TPA-OH:NaOH:H_2O =1:56:14:7714, respectively. Then, the β-SiC support was placed in the solution. The nanoscopic layer of silica of the β-SiC support provides the silicon source, thus inducing a substrate self-transformation following the strategy developed elsewhere.[23,24] The synthesis was performed at 170 °C under autogenous pressure. The synthesis duration was varied between 72 and 670 h. After hydrothermal synthesis, the solid material was dried at 100 °C. The organic template was removed by treating the material in air at 500 °C for 5 h. The composite was then ion-exchanged with an aqueous 1 mol L^{-1} NH_4Cl

(20) Calis, H. P. A.; Gerritsen, A. W.; van den Bleek, C. M.; Legein, C. H.; Jansen, J. C.; van Bekkum, H. *Can. J. Chem. Eng.* **1995**, *73*, 120−128.
(21) Seiger, G. B. F.; Oudshoorn, O. L.; Boekhorst, A.; van Bekkum, H.; van den Bleek, C. M.; Calis, H. P. A. *Chem. Eng. Sci.* **2001**, *56*, 849−857.
(22) Mintova S.; Valtchev V.; Konstantinov L.; *Zeolites* **1996**, *17*, 462−465.
(23) Sterte J.; Hedlung J.; Creaser D.; Ohrman O.; Zheng W.; Lassinantti M.; Li Q.; Jareman F. *Catal. Today* **2001**, *69*, 323−329.
(24) Louis B.; Tezel C.; Kiwi-Minsker L.; Renken A. *Catal. Today* **2001**, *69*, 365−370.
(25) Lai, R.; Yan, Y.; Gavalas, G. R. *Microporous Mesoporous Mater.* **2000**, *37*, 9−19.
(26) Valtchev, V.; Mintova, S.; Schoeman, B.; Spasov, L.; Konstantinov, L. *Zeolites* **1995**, *15*, 527−532.
(27) Ulla, M. A.; Mallada, R.; Coronas, J.; Gutierrez, L.; Miro, E.; Santamaria, J. *Appl. Catal. A* **2003**, *253*, 257−269.
(28) Ulla, M. A.; Miro, E.; Mallada, R.; Coronas, J.; Santamaria, J. *Chem. Commun.* **2004**, 528−529.
(29) Ledoux, M. J.; Guille, J.; Hantzer, S.; Dubots, D. U.S Patent 4914070, Pechiney, 1990.
(30) Ledoux, M. J.; Pham-Huu, C. *Cattech* **2001**, *5*, 226−246.
(31) Ledoux, M. J.; Pham-Huu, C. *Catal. Today* **1992**, *15*, 263−284.
(32) Louis, B.; Kiwi-Minsker, L.; Renken, A. *Recents Prog. Genie Procedes* **2001**, *15*, 443−450.
(33) Lee, J. S.; Lee, Y. J.; Tae, E. L.; Park, Y. S.; Yoon, K. B. *Science* **2003**, *301*, 818−821.
(34) Wang, H.; Wang, Z.; Huang, L.; Mitra, A.; Yan, Y. *Langmuir* **2001**, *17*, 2572−2574.
(35) Song, W.; Grassian, V. H.; Larsen, S. C. *Microporous Mesoporous Mater.* **2006**, *88*, 77−83.
(36) Patcas, F. C. *J. Catal.* **2005**, *231*, 194−200.

solution (100 mL) for 16 h at 80 °C and was subsequently calcined at 500 °C for 5 h to produce the H-form of the zeolite.

Fluoride-Mediated Route. The synthesis mixture was prepared by dissolving the organic template (TPABr, 98%, Aldrich Chemie) in deionized water and by stirring for 10 min. The precursor solution was achieved by stirring the mixture after an addition of ammonium fluoride (NH_4F, 98%, Fluka) for 15 min. Then, sodium aluminate ($NaAlO_2$, Riedel de Häen) was added and the solution was stirred for another 15 min. The reactants were mixed according to the following composition: $NaAlO_2$:TPA-Br:NH_4F:H_2O = 1:6:184:6538, respectively. A few drops of hydrofluoric solution (40 wt %) were added to decrease the alkalinity of the solution to pH = 5. Then, the β-SiC support was placed in the solution, and the solution was aged for 3 h. The silica nanoscopic surface layer on β-SiC support serves as a nutrient for the silicon source. The synthesis was performed at 165 °C under autogenous pressure for 147 h. After hydrothermal synthesis, the solid material was dried at 100 °C. Afterward, the organic template and ammonia were removed by treating the material in air at 500 °C for 5 h.

Characterizations. Specific surface areas (SSA) of the different materials were determined by N_2 adsorption−desorption measurements at 77 K by employing the Brunauer−Emmet−Teller (BET) method (Micromeritics sorptometer Tri Star 3000). Prior to N_2 adsorption, the sample was outgassed at 300 °C for 4 h to desorb water and moisture adsorbed on the surface and inside the porous network.

X-ray diffraction patterns (XRD) were recorded on a Brucker D8 Advance diffractometer with a VANTEC detector side and Ni filtered Cu Kα radiation (1.5406 Å) over a 2θ range of 5−50° and a position sensitive detector using a step size of 0.02° and a step time of 2 s.

Scanning electron microscopy (SEM) micrographs were recorded on a JEOL FEG 6700F microscope working at 9 kV accelerating voltage. Before observation, the sample was covered by a carbon layer to decrease the charge effect during the analysis. For transmission electron microscopy (TEM) measurements, the sample was first ultrasonically dispersed in an ethanol solution and a drop was deposited on a copper grid with a perforated carbon film and was rapidly transferred to a Topcon UHR 002B microscope and was operated at 200 kV with a point-to-point resolution of 0.17 nm. The Si/Al ratio was determined by elemental analysis coupled with the TEM chamber.

^{27}Al (I = 5/2) magic-angle spinning nuclear magnetic resonance (MAS NMR) was carried out on a Brucker DSX 400 spectrometer operating at B_0 = 9.4 T (Larmor frequency ν_0 = 104.2 MHz). A single pulse of 0.7 μs with a recycle delay of 300 ms was used for all experiments. The spinning frequency was 10 kHz. Measurements were carried out at room temperature with $[Al(H_2O)_6]^{3+}$ as external standard reference. ^{29}Si MAS NMR was carried out on a Brucker MSL 300 spectrometer operating at B_0 = 7.04 T.

The Brönsted acidity of the materials was evaluated by using an H/D isotope-exchange technique, which counts the number of O−H groups, as reported elsewhere.[37] This technique also allows the determination of the chemical composition of the as-synthesized composite material (Si/Al ratio, unit cell formula).

Catalytic Test. The sample of as-grown zeolite nanofibers (140 h) has been tested in the reaction of methanol to gasoline (MTG). The reaction was performed at atmospheric pressure and 400 °C using a fixed-bed quartz reactor packed with 4 g of catalyst and a mixture of 0.5 mL min^{-1} methanol and 60 mL min^{-1} argon. The methanol was fed by means of high-performance liquid chromatography (HPLC) pump, followed by vaporization at 150 °C in argon flow. The analyses were performed by gas chromatography to quantify the concentration of hydrocarbons with an FID detector and DB-1 column (30-m long and 0.53-mm internal diameter). The temperature was controlled by means of two thermocouples placed inside and outside the reactor system.

(37) Louis, B.; Walspurger, S.; Sommer, J. *Catal. Lett.* **2004**, *93*, 81−84.

Results and Discussion

Zeolite Nanofibers/β-SiC Composite. The SEM micrographs of as-synthesized materials on β-SiC extrudates as a function of the synthesis duration are presented in Figure 2. The color of the β-SiC substrate changed from gray to light gray after the synthesis, indicating a modification of the surface, probably via the coverage by a new material. By elemental analysis of this new material with Energy-Dispersive X-ray Analysis (EDAX), a Si/Al ratio of 30 was found, thus confirming Al introduction.

The low-magnification SEM micrograph of this alumino-silica material clearly evidenced the formation of a dense weblike network of nanowires after synthesis duration of 140 h (Figure 2a and 2b).

Statistical SEM analysis showed that the formed nanowires have an extremely high homogeneity in diameter, 90 nm, with lengths up to tenths of micrometers leading to a high surface-to-volume ratio. The presence of a few crystals can also be detected (Figure 2c). According to the SEM observations, one could state that a peculiar zeolite morphology was obtained, while using a Si source chemically attached on the macroscopic host structure, indicating a different nucleation and growth mechanism.

These alumino-silica nanowires are extremely straight which indicate a preferential direction during the nucleation and growth process. A longer synthesis duration (335 h) led to the formation of some alumino-silicate nanoparticles on the top of the former nanowire network (Figure 2d).

In some regions, numerous nanowires were found to be encapsulated within a crystal (Figure 2e). A further prolongation of the synthesis, up to 670 h, led to the transformation of the nanowires into rectangular films (μ-scale). These films are present in the form of large plates (Figure 2f), which result from the aggregation of individual nanowires (Figure 2f inset) as already observed by Song et al.[35]

These results indicate that the zeolite nanowires, observed after a short synthesis time (140 h), consist in a metastable phase and slowly merge together to yield a more stable phase such as crystallites with a lower surface energy constraint. Figure 3 also evidenced the self-assembly of individual nanocrystals into 1D nanowires, thus playing the role of starting building blocks for a microscale organization. The self-assembly into nanofibers can be due to a thermoconvective instability of Bénard-Marangoni type, induced by a higher rate of solvent evaporation compared to the rate of crystal formation.[35] Hence, the local conditions (temperature, water pressure, nutrient concentrations) probably induced an isothermal heating-evaporation-induced self-assembly effect (IHEISA).[38]

The TEM image further supports the regular nanofibrous structure (90 nm in diameter) of the as-synthesized material (Figure 4). The nanowire appears to be extremely thin, taking into account the clear density contrast observed in the TEM image. Combination of SEM and TEM analyses led to a statement that the 1D material synthesized belongs to a nanoribbon rather than a nanowire, owing to its low thickness. The presence of holes inside the material could also be related to the competitive process of dissolution by holes nucleation.

The preparation of zeolite BEA nanofibers has already been performed via epitaxial growth on preshaped SSZ-31 nanofi-

(38) Wong, S.; Kitaev, V.; Ozin, G. A. *J. Am. Chem. Soc.* **2003**, *125*, 15589−15598.

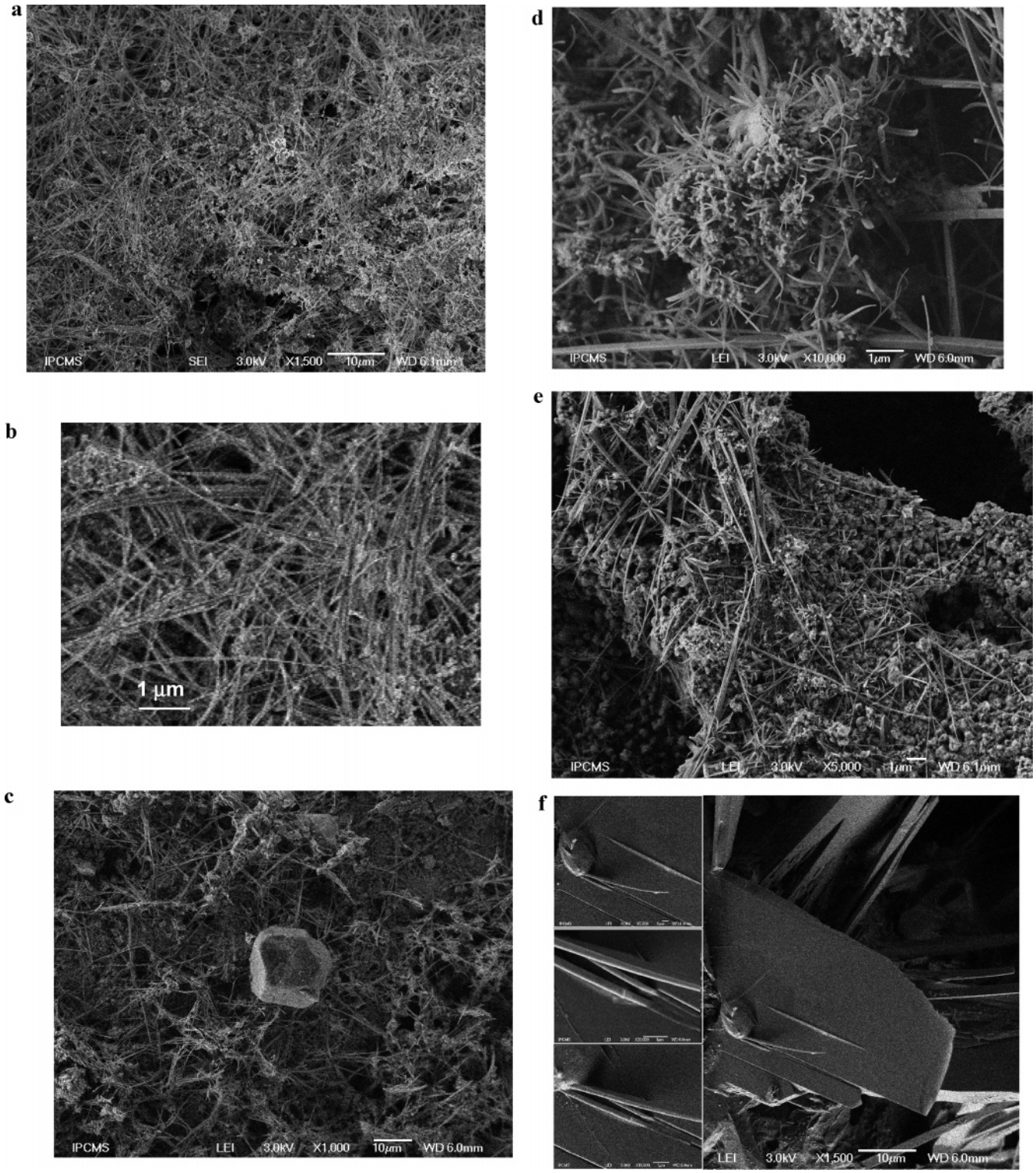

Figure 2. SEM images of alumino-silica nanowires grown on SiC as a function of the synthesis duration 140 h (a−c); 335 h (d, e); 670 h (f).

bers.[39] The following question then arises: are these as-synthesized self-assembled nanofibers zeolitic material?

The SSA was increased from 19 m^2/g for the bare β-SiC foam support to 55 m^2/g for the nanofibers/β-SiC composite (after 140 h of synthesis). Moreover, this increase in the SSA values was connected with the generation of micropores, which are absent in the bare β-SiC support, but are typical for zeotype materials. Since a powdered MFI-type zeolite prepared with the same gel composition possess a SSA = 320 m^2/g, the layer of alumino-silicate deposited was estimated to 12 wt %.

The crystallinity of the different alumino-silica coatings was investigated by means of powder XRD technique. Figure 5 presents the diffraction patterns after synthesis durations ranging between 72 and 335 h. It appears that the alumino-silica nanofibers grown during 72 h exhibit the crystallinity of MFI structure (Figure 5a), thus indicating the formation of ZSM-5

(39) Nair, S.; Villaescusa, L. A.; Camblor, M. A.; Tsapatsis, M. *Chem. Commun.* **1999**, 921−922.

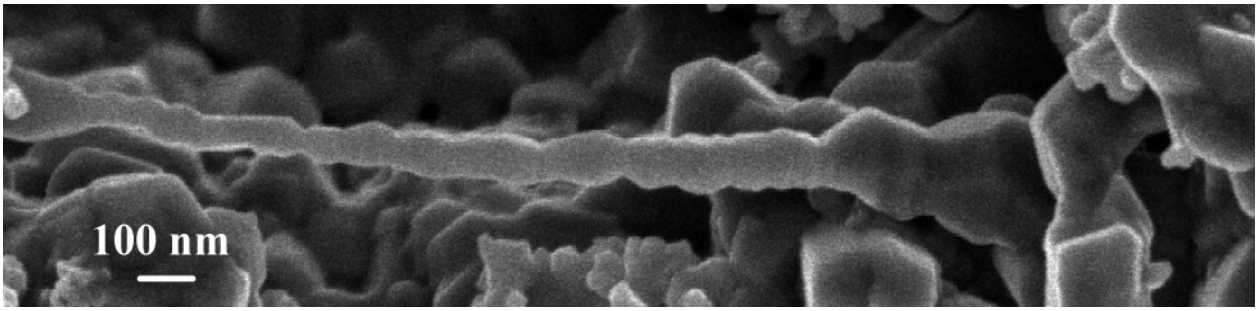

Figure 3. High-resolution SEM micrograph of alumino-silica nanowires (synthesis time: 140 h) forming by the assembly of individual nanocrystals along the growth axis.

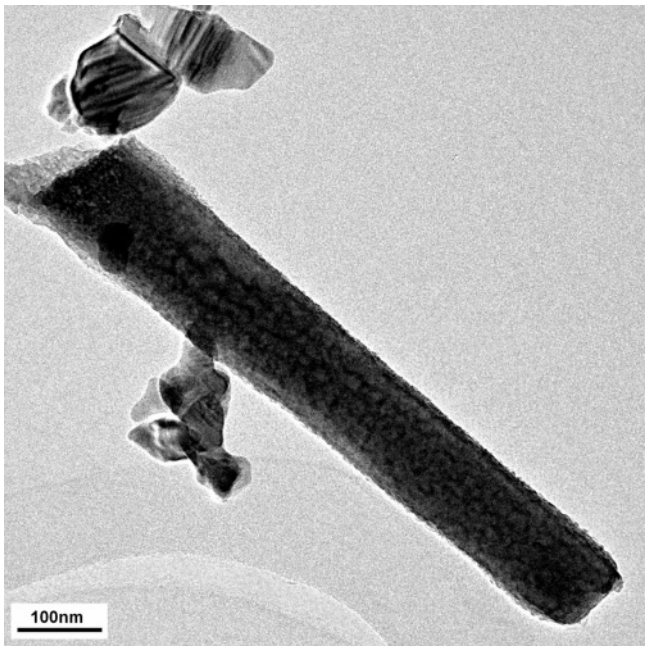

Figure 4. TEM image of alumino-silica grown nanofibers on SiC after 140 h.

zeolite.[40] However, with an increase of the synthesis duration, the crystallinity decreased drastically (Figure 5b and 5c). These XRD patterns are characteristic of as-called "X-ray amorphous zeolites".[41,42] This secondary amorphous phase has many compositional and chemical similarities to the parent zeolite but is lacking in long-range order.[43] Such amorphization process can be due to partial dissolution of the formed zeolite under hydrothermal conditions. The zeolite formation is a fine balance between crystal growth, that is, nuclei formation and crystal dissolution (holes nucleation). As a function of the synthesis duration, the nature of the products closely moves toward the next stable product and so on, as a function of this formation−dissolution process. Another possible pathway is the formation of a layered structure as an intermediate, which leads directly to the zeolite.[44] However, the diffractogram 5d confirms the presence of MFI zeolite after 335 h of synthesis, since the powdered material detached from the support presents the typical diffraction lines of ZSM-5 zeolite. The silica outer layer of the β-SiC substrate has been converted via self-transformation into MFI zeolite. After dissolution of the crystals, recrystallization occurs, leading to the same zeolite structure with, however, a slightly different morphology as observed by SEM images (Figure 2). Apparently, the use of silica covalently bonded to the SiC surface allows us to successfully synthesize some metastable zeolite phases, which are unstable in the reaction medium.

The ^{27}Al and ^{29}Si MAS NMR spectra of the final material prepared during 670 h are shown in Figure 6a and 6b, respectively. A single and narrow signal was observed at 52 ppm (Figure 6a), which can unambiguously be attributed to tetrahedrally coordinated aluminum atoms in the zeolite framework.[45] Furthermore, the absence of any signal at 0 ppm indicates the absence of any extraframework aluminum species. Indeed, all aluminum atoms were successfully incorporated into the MFI zeolite framework. Figure 6b presents the ^{29}Si MAS NMR spectrum and shows one major peak at −111 ppm. A small shoulder centered at −102 ppm was also observed. These peaks can be assigned to Q_4 and to Q_3 structures, respectively.[46] These ^{29}Si and ^{27}Al NMR spectra further confirm the presence of a zeolite framework containing both AlO_4 and SiO_4 tetrahedra (Si/Al = 20).

The zeolite acid properties are directly related to its aluminum content. Therefore, the Brönsted acidity of the different zeolite/β-SiC composites was investigated by means of H/D isotope exchange technique,[37,47] and the results are presented in Table 1. The bare β-SiC substrate exhibits only a limited amount of OH groups, 0.110 mmol g_{SiC}^{-1}. After a synthesis duration of 140 h, the total number of Brönsted acid sites was increased to 0.414 mmol $g_{composite}^{-1}$. The acidity of the material synthesized for 335 h was decreased which is in agreement with a crystallization−dissolution process as suspected from XRD measurements. The MFI zeolite prepared after 670 h possess 0.208 mmol OH groups $g_{composite}^{-1}$. A quantity of 0.616 mmol OH groups/$g_{zeolite}$ was measured on the powder scratched from the support surface. Hence, on the basis of H/D exchange experiments, the amount of zeolite nanofibers present on the β-SiC support is 15 wt %. This value is in line with the increase in the SSA values which led to an estimation of 12 wt % of zeolite present in the final composite. This H/D exchange

(40) Koningsveld, H.; van Bekkum, H.; Jansen, J. C. *Acta Crystallogr.* **1987**, *34B*, 127−133.
(41) Jacobs, P. A.; Derouane, E. G.; Weitkamp, J. *J. Chem. Soc., Chem. Commun.* **1981**, 591−593.
(42) Schlenker, J. L.; Peterson, B. K. *J. Appl. Crystallogr.* **1996**, *299*, 178−185.
(43) Cundy, C. S.; Cox, P. A. *Microporous Mesoporour Mater.* **2005**, *82*, 1−78.
(44) Lohse, U.; Altrichter, B.; Fricke, R.; Pilz, W.; Schreier, E.; Garkisch, C.; Jancke, K. *J. Chem. Soc., Faraday Trans.* **1997**, *93*, 505−512.
(45) *High-Resolution Solid State NMR of Silicates and Zeolites*; Engelhardt, G., Michel, D., Eds.; John Wiley and Sons: Chichester, U.K., 1997.
(46) *Multinuclear Solid-State NMR of Inorganic Materials*; Mac Kenzie, K. J. D., Smith, M. E., Eds.; Pergamon Materials Series, vol. 6; Pergamon: Oxford, U.K., 2002.
(47) Tessonnier, J. P.; Louis, B.; Walspurger, S.; Sommer, J.; Ledoux, M. J.; Pham-Huu, C. *J. Phys. Chem. B* **2006**, *110*, 10390−10395.

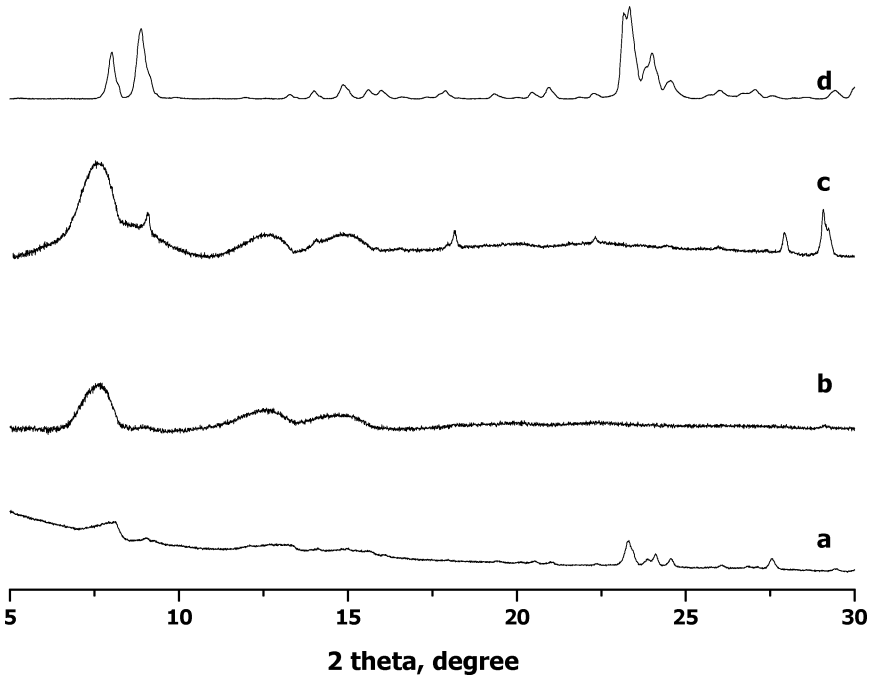

Figure 5. XRD patterns of the as-grown aluminosilica nanofibers on SiC after different synthesis durations: (a) 72 h, (b) 140 h, and (c) 335 h. (d) Powder detached from the support after 335 h.

technique allows a precise quantification of the Brönsted acid sites, thus leading to the determination of the Si/Al ratio in case the zeolite structure is known.[47] From the XRD data (Figure 5d), it appears that the formed zeolite belongs to the MFI structure. A quantity of 0.616 mmol OH group/g_{ZSM-5} corresponds to a Si/Al = 26,[48] thus supporting the elemental analysis results (Si/Al = 30). Hence, the H/D exchange measurements prove again the presence of ZSM-5 zeolite on the silicon carbide substrate. The mechanical anchorage of the as-synthesized zeolite on the SiC surface was checked by submitting the composite to a sonication treatment for 30 min. No zeolite loss was observed after such treatment (SSA measurements). Similar results have already been observed on conventional ZSM-5 and BEA zeolites coated on the SiC surface.[9,10] The strong mechanical anchorage of as-grown zeolite was explained by the existence of a covalent bond between the SiO_x layer on SiC and the zeolite.

Catalytic Activity in the Methanol-to-Gasoline Reaction. The catalytic activity of the composite HZSM-5 nanofibers/β-SiC (140 h) was investigated in the conversion of methanol into hydrocarbons.[49−52] The steady-state conversion of methanol was reached after 2 h and was about 38% (Figure 7).

Under similar experimental conditions, Zaidi and Pant have found the same level of conversion with an industrial HZSM-5 zeolite.[53] The selectivity toward the reaction products is shown in Figure 8. During the first 2 h of the reaction, the ZSM-5/SiC composite exhibited very high selectivity (between 85 and 90%) toward saturated hydrocarbons with more than five carbon atoms chain length (C_{5+}). This composite made of zeolite nanofibers appears to be an active and selective (at least during 2 h) catalyst for the MTG reaction. However, after the initial period, the selectivity dramatically changed toward light-saturated hydrocarbons C_1-C_4 fraction (98% after 6 h of reaction). Surprisingly, no products in the range C_5-C_9 can be detected after 6 h, but only C_{10}, C_{11}, and C_{12} were present. This phenomenon, which is limited in our study, the so-called "window effect", has been observed by Gorring for zeolites with smaller cages.[54a] Recently, Ruthven has attributed such distribution among the products to beneficial heat transfer for $C_{10}-C_{12}$ alkanes.[54b]

These ZSM-5 nanofibers grown and self-assembled onto parent SiC support are active in the MTG reaction, thus confirming the acidity of the material. The reason for such selectivity change during the course of reaction has not been fully understood yet. However, it is possible to anticipate the changes in the zeolite channel accessibility, similarly to that observed during the methane dehydroaromatization reaction over the ZSM-5 catalyst. In the present work, the change in selectivity toward the products is probably connected to micropore plugging via acidic condensation by hydrocarbon deposits, which can undergo isomerization-cracking reactions (mainly C_1-C_4 formed) in agreement with the "carbon pool mechanism".[50,52]

Tentative Mechanism of Zeolite ZSM-5 Nanofibers Growth. The generally accepted model of Barrer et al.[55] supposes that the formation of the zeolite crystals occurs in solution, that is, the nucleation and growth of crystalline nuclei are a result of condensation reactions between soluble species. The gel plays only a limited role, acting as a reservoir of matter. However, in our in-situ procedure, where the silica source is provided by the support surface containing oxygen−silicon species, one can presume a reorganization of the gel via solid−solid transformations.[56] Ravishankar and co-workers have concentrated their

(48) *Atlas of zeolite structure types*; Meier, W. M., Olson, D. H., Eds.; Butterworth: London, 1992.
(49) Chang, C. D. *Catal Rev. Sci. Eng.* **1983**, *25*, 1−118.
(50) Stöcker, M. *Microporous Mesoporous Mater.* **1999**, *29*, 3−48.
(51) Froment, G. F.; Dehertog, W. J. H.; Marchi, A. J. *Catalysis* **1992**, *9*, 1−64.
(52) Haw, J. F.; Nicholas, J. B.; Song, W.; Deng, F.; Wang, Z.; Xu, T.; Heneghan, C. S. *J. Am. Chem. Soc.* **2000**, *122*, 4763−4775.
(53) Zaidi, H. A.; Pant, K. K. *Catal. Today* **2004**, *96*, 155−160.
(54) (a) Gorring, R. L. *J. Catal.* **1973**, *31*, 13−26. (b) Ruthven, D. M. *Microporous Mesoporous Mater.* **2006**, *96*, 262−269.
(55) Barrer, R. M.; Buynham, J. W.; Bultitude, F. W.; Meier, W. M. *J. Chem. Soc.* **1959**, 195−208.

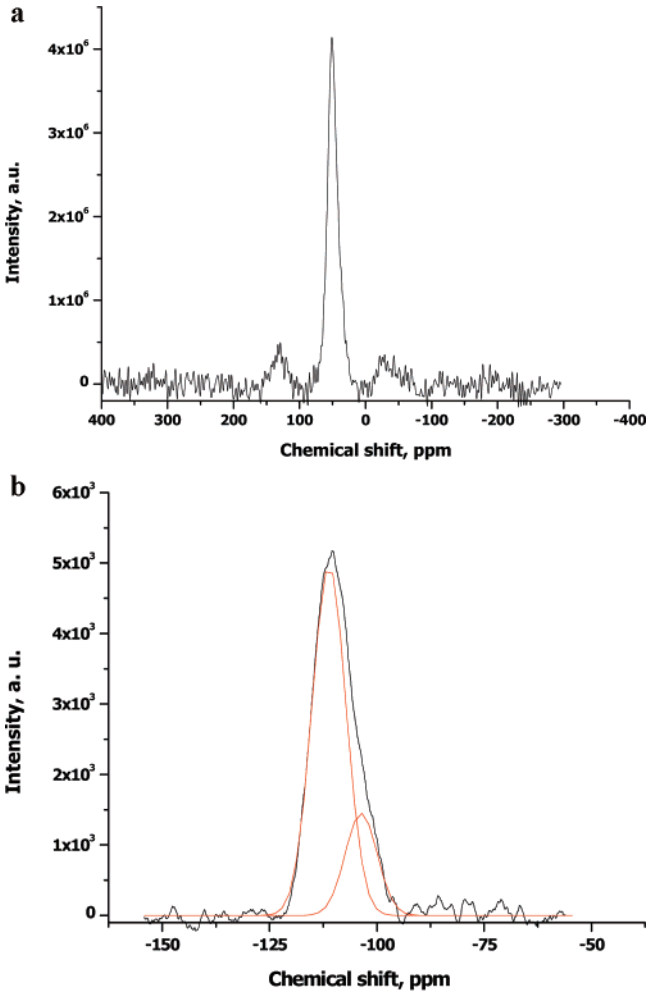

Figure 6. (a) ^{27}Al and (b) ^{29}Si MAS NMR spectra of zeolite nanowires (670 h) showing the presence of AlO_4 and SiO_4 tetrahedra species which are typical for zeolites.

Table 1. Titration via H/D Isotope Exchange Technique of the Number of OH Groups Present on the Different Zeolite/SiC Composites

sample	number of O–H groups [mmol g^{-1}]
β-SiC	0.110
fibers 140 h	0.414
fibers 335 h	0.182
fibers 670 h	0.208
powder 670 h	0.616

studies in a detailed characterization of the MFI precursor and thus have identified the constituent "nanoslabs"[57−60] with few nanometers in size. The aggregation of these nanoslabs leads to larger particles and ultimately to the final crystal. The formation of zeolite nanofibers in the present study seems to involve an aggregation mechanism on the basis of a layer-by-layer Gibbs−Volmer growth mode.[61] A growth unit is adsorbed on the growing (nano)crystal face and migrates to find its optimum location.

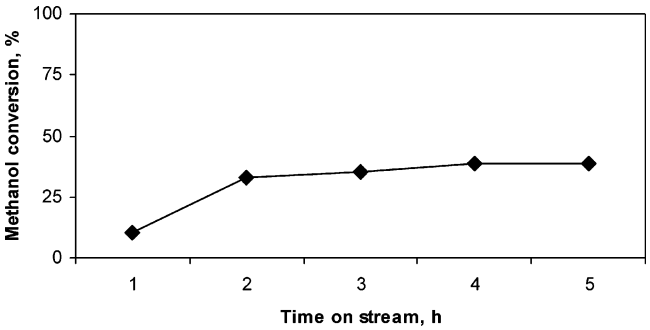

Figure 7. Activity of HZSM-5/SiC (670 h) in the conversion of methanol to hydrocarbons (MTG) at 400 °C.

However, it is generally admitted that there is a geometrical tuning between the template cations and the silica channel system. Burkett and Davis gave evidence of the existence of van der Waals interactions between quaternary ammonium cations and the inorganic silica species,[62] thus inducing the assembly of these organomineral entities and the growth of the nuclei. A template cation is envisaged as being attached at the surface site of amorphous silica particle. Monomer units from the solution then join the growth site and assemble in an ordered array. In spite of global repulsive energy barriers for an aggregation model, Kirschhock et al. have calculated a net attractive energy minimum at 0.7 nm from the substrate surface.[60] Hence, the aggregate may behave as a nutrient-recipient pair in consistency with Thompson's "tugging-chain" mechanism.[63]

The experimental factors which govern the self-assembly of zeolite nanocrystals into fibers or thin films are not well understood yet. Nevertheless, the T−O−T bond making and bond breaking (where T = Si or Al), on the basis of nucleophilic reactions, facilitate structural modification catalyzed by hydroxyl ions. The use of the fluoride ion as mineralizer instead of the conventionally used hydroxide ion has presented a significant breakthrough in the field of zeolite synthesis.[64−68] The mineralizing strength of F^- is less than that of OH^-, so the solubilities and effective supersaturations are lower. Figure 9 shows the SEM micrograph of the zeolite nanocrystals belonging to the RTH topology[69] from the synthesis performed under acidic conditions (pH = 5) as described in section 2. The autoassembly of these nanocrystals produced neither nanofibers nor continuous films but zeolite crystals, thus supporting an effect of the mineralizer nature over the growth mode and final structure.

(56) Derouane, E. G.; Detremmerie, S.; Gabelica, Z.; Blom, N. *Appl. Catal.* **1981**, *1*, 201−224.
(57) Ravishankar, R.; Kirschhock, C. E. A.; Schoeman, B. J.; Vanoppen, P.; Grobet, P. J.; Storck, S.; Maier, W. F.; Martens, J. A.; de Schryver, F. C.; Jacobs, P. A. *J. Phys. Chem. B* **1998**, *102*, 2633−2639.
(58) Ravishankar, R.; Kirschhock, C. E. A.; Knops-Gerrits, P. P.; Feijen, E. J. P.; Grobet, P. J.; Vanoppen, P.; de Schryver, F. C.; Miehe, G.; Fuess, H.; Schoeman, B. J.; Jacobs, P. A.; Martens, J. A. *J. Phys. Chem. B* **1999**, *103*, 4960−4964.
(59) Kirschhock, C. E. A.; Ravishankar, R.; Verspeurt, F.; Grobet, P. J.; Jacobs, P. A.; Martens, J. A. *J. Phys. Chem. B* **1999**, *103*, 4965−4971.
(60) Kirschhock, C. E. A.; Ravishankar, R.; Jacobs, P. A.; Martens, J. A. *J. Phys. Chem. B* **1999**, *103*, 11021−11027.
(61) *Kinetik der Phasenbildung*; Volmer, M., Ed.; Steinkopff: Dresden, Germany, 1939.
(62) Burkett, S. L.; Davis, M. E. *J. Phys. Chem.* **1994**, *98*, 4647−4653.
(63) *Molecular Sieves*; Thompson, R. W., Karge, H. G., Weitkamp, J., Eds.; Springer-Verlag: Berlin, 1998.
(64) Flanigen, E. M.; Patton, R. L. U.S. Patent 4073865, 1978.
(65) Guth, J. L.; Kessler, H.; Higel, J. M.; Lamblin, J. M.; Patarin, J.; Seive, A.; Chezeau, J. M.; Wey, R. *Zeolite synthesis*; ACS Symposium Series No. 398; American Chemical Society: Washington, DC, 1989; pp 176−182.
(66) Camblor, M. A.; Villaescusa, L. A.; Diaz-Cabanas, M. J. *Top. Catal.* **1999**, *9*, 59−76.
(67) Louis, B.; Kiwi-Minsker, L. *Microporous Mesoporous Mater.* **2004**, *74*, 171−178.
(68) Axon, S. A.; Klinowski, J. *J. Chem. Soc., Faraday Trans.* **1990**, *86*, 3679−3682.
(69) Wagner, P.; Nakagawa, Y.; Lee, G. S.; Davis, M. E.; Elomari, S.; Medrud, R. C.; Jones, S. I. *J. Am. Chem. Soc.* **2000**, *122*, 263−285.

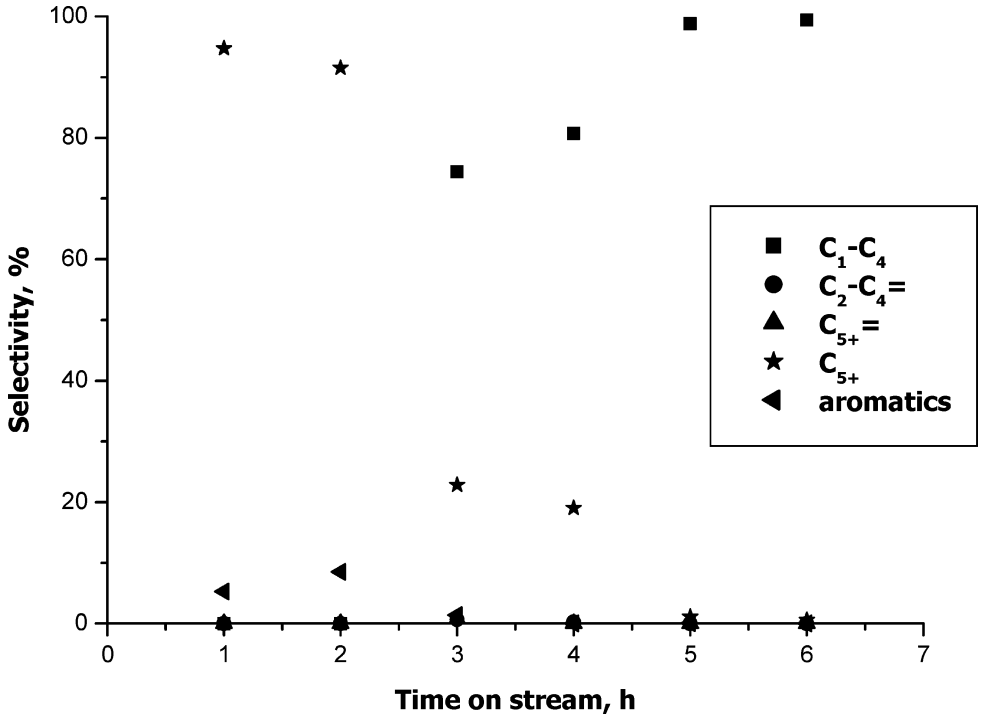

Figure 8. Selectivity toward the different products (HZSM-5/SiC, 670 h) at 400 °C. The product selectivity modification as a function of time on stream clearly indicates the change in the zeolite porous network.

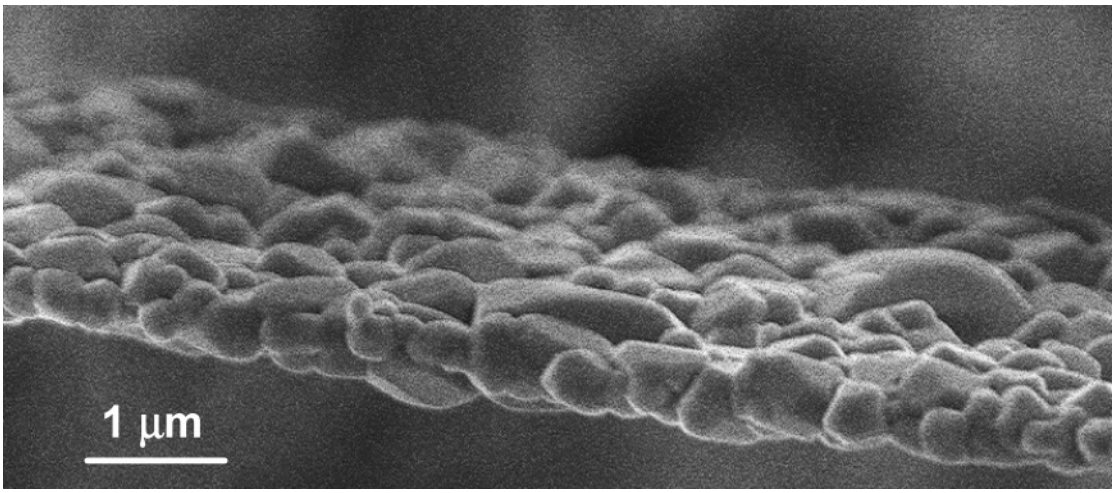

Figure 9. SEM micrograph of zeolite autoassembled nanocrystals grown on SiC via fluoride-mediated synthesis (147 h).

Furthermore, it appears that this innovative strategy of using the self-transformation of the bare β-SiC support allows the formation of zeolite nanocrystals, which can grow in peculiar and tailorable directions and manner depending on the operating conditions (pH, mineralizer, time, temperature, concentration). Whereas previous studies reported the use of covalent linkers,[70,71] proteins,[72,73] or organic acids[74] to guide the assembly of zeolite crystals, we have successfully demonstrated that zeolite nanocrystals can, by themselves, build a nanofibrous network. Finally, our approach can open new routes toward the synthesis of novel zeolite structures and hence a combination of their nano/microorganization on a macroshaped support surface.

Conclusion

Zeolite nanofibers with a regular size of 90 nm and lengths of micrometers were prepared for the first time via in-situ silicon carbide support self-transformation. The aggregation degree of the zeolite nanofibers has been tuned by change of the synthesis duration, the pH, and the nature of the mineralizer (OH^- or F^-). The different characterization techniques have shown that these nanofibers exhibited the MFI structure together with the typical acidity of ZSM-5 zeolite. Moreover, this ZSM-5/β-SiC composite was active in the methanol-to-gasoline process.

(70) Ha, K.; Lee, Y. J.; Lee, J. H.; Yoon, K. B. *Adv. Mater.* **2000**, *12*, 1114−1117.
(71) Yan, Y.; Bein, T. *J. Phys. Chem.* **1992**, *96*, 9387−9393.
(72) Um, S. H.; Lee, G. S.; Lee, Y. J.; Koo, K. K.; Lee, C.; Yoon, K. B. *Langmuir* **2002**, *18*, 4455−4459.
(73) Jung, J. H.; Ono, Y.; Hanabusa, K.; Shinkai, S. *J. Am. Chem. Soc.* **2000**, *122*, 5008−5009.
(74) Cho, G.; Lee, J. S.; Glatzhofer, D. T.; Fung, B. M.; Yuan, W. L.; O'Rear, E. A. *Adv. Mater.* **1999**, *11*, 497−499.

In conclusion, we describe a novel synthesis route based on two important findings: (1) a β-SiC material self-transformation into a zeolitic material without any extra addition of silica source, (2) the autoassembly of the zeolite nanocrystals into long nanofibers without any chemical binder use (neither organogelator nor halogenosilanes).

Finally, merging the huge number of zeolite structures (existing or to be discovered), the numerous possibilities to modify the synthesis conditions (pH, concentration, temperature), and the type of silica-containing substrates known offer an extremely high degree of freedom for engineering new composites with properties specifically tailored for defined applications. The zeolite/SiC composite can also be synthesized with various shapes and sizes depending on the downstream applications.

Acknowledgment. The authors are grateful to Drs. Severinne Rigolet (LMPC, UMR 7016), T. Dintzer, and J.P. Tessonnier (LMSPC) for NMR and EM measurements. Degussa AG (Business Unit Aerosil & Silanes) is acknowledged for kindly providing silica and alumina sources. Sicat (Otterswiller, France) is kindly acknowledged for the supply of the SiC materials.

JA0686209